Numerical analysis for a discontinuous rotation of the torus

Bruin, H.; Lambert, A.; Poggiaspalla, G.; Vaienti, S.

Published in:
Chaos

DOI:
10.1063/1.1572411

Publication date:
2003

Numerical analysis for a discontinuous rotation of the torus

H. Bruin, A. Lambert, G. Poggiaspalla, and S. Vaienti

Citation: Chaos **13**, 558 (2003); doi: 10.1063/1.1572411
View online: https://doi.org/10.1063/1.1572411
View Table of Contents: http://aip.scitation.org/toc/cha/13/2
Published by the American Institute of Physics

Numerical analysis for a discontinuous rotation of the torus

H. Bruin[a)]
Department of Mathematics, University of Groningen, Groningen, The Netherlands

A. Lambert[b)] and G. Poggiaspalla[c)]
Centre de Physique Théorique, CNRS Luminy, Case 907, F-13288 Marseille Cedex 9, France and Université d'Aix-Marseille II and FRUMAM (Fédération de Recherche des Unités de Mathématiques de Marseille), France

S. Vaienti[d)]
Centre de Physique Théorique, CNRS Luminy, Case 907, F-13288 Marseille Cedex 9, France and PHYMAT, Université de Toulon et du Var and FRUMAM (Fédération de Recherche des Unités de Mathématiques de Marseille), France

(Received 11 July 2002; accepted 17 March 2003; published 21 May 2003)

In this paper, we study a class of piecewise rotations on the square. While few theoretical results are known about them, we numerically compute box-counting dimensions, correlation dimensions and complexity of the symbolic language produced by the system. Our results seem to confirm a conjecture that the fractal dimension of the exceptional set is two, as well as indicate that the dynamics on it is not ergodic. We also explore a relationship between the piecewise rotations and discretized rotations on lattices $\mathbb{Z}^{2n}$. © *2003 American Institute of Physics.*
[DOI: 10.1063/1.1572411]

It is well known that simply defined dynamical systems can exhibit very complex behavior. In this paper we will consider a family of piecewise isometries, namely of discontinuous rotations on the two-torus. These systems are not ergodic; their various invariant sets display a rich and complicated geometry and support dynamics with nontrivial statistical properties. Most of the characteristics of these systems are not completely understood. Basic questions such as the distribution of periodic points and the coding of the trajectories on the closure of the discontinuity lines, are still open. We will present a careful numerical investigation of three features of these maps. First, we compute the fractal dimension of the exceptional set (i.e., the complement of the collection of ''periodic islands''). There is evidence that this exceptional set may have a positive Lebesgue measure. Second, we investigate the complexity of the orbits on the exceptional set; we found several (piecewise) polynomial behaviors of the complexity function, some referring to a substitution system. Third, we show a correspondence between discontinuous rotations of the torus and discretized rotations on a lattice. This correspondence may help in explaining the differences in the growth of the complexity function.

I. INTRODUCTION

In this paper, we present numerical studies on a class of piecewise isometries on a two-dimensional compact manifold (the square or the two-torus). These maps arise from different situations.

(a) They emerge in the study of overflow behavior for a class of digital filters. Historically, this was the first situation where they were introduced and numerically studied.[1]
(b) They are realizations of discontinuous automorphisms of the torus which preserve the Lebesgue measure; in particular they are the piecewise linear versions of the well-known standard map.
(c) They are closely related to systems representing round-off schemes emerging from the numerical simulation of dynamical systems, e.g., Refs. 2 and 3.
(d) They serve as a conjugate model for the first return maps of certain dual billiard systems.[4]

These maps give rise to a complicated interplay between regular (periodic or quasi-periodic) motion and abundant erratic regions whose ergodic and statistical descriptions are far from being understood. Roughly speaking the torus splits into three invariant sets: the discontinuity line and its forward and backward images, the set of periodic points surrounded by (quasi-)periodic circles and the complement Δ' of these two sets. Despite the simple form of the isometries, the existence and the nature of these three sets raise several questions. For example, are there periodic orbits of arbitrarily large period? What is the topological and geometric structure of Δ'? Does Δ' admit dense orbits? Apart from a few cases quoted below, these questions are completely open.

We briefly discuss the main rigorous contributions to this field. Goetz in Refs. 5–7, gave some general results on the coding and the geometry of the periodic cells. An exhaustive study of three examples can be found in Refs. 8 and 9 by using intricate renormalization techniques, the authors were able to characterize the set of periodic points and the

[a)]Electronic mail: bruin@math.rug.nl
[b)]Electronic mail: lambert@cpt.univ-mrs.fr
[c)]Electronic mail: poggiasp@cpt.univ-mrs.fr
[d)]Electronic mail: vaienti@cpt.univ-mrs.fr

dynamics on Δ'. A generalization of their techniques to other cases seems to be very hard. A related, more arithmetic analysis of the periodic sets can be found in Refs. 2 and 3. The topological entropy of piecewise isometries was shown to be zero in dimension 2 in Ref. 10 and in arbitrary dimension in Ref. 11. Parallel to these analytic works, there have been several numerical investigations; they usually confirmed, in a large variety of situations, the rich behavior quoted above, but also revealed new features like the presence of invariant curves in Δ', which suggests that the dynamics is not transitive on the exceptional set[12] and the unboundedness of return times to some subsets of the space. In this paper we focus on the example studied in Ref. 8. This system, as we will see in the next section, is a piecewise rotation depending on one parameter, the angle θ. Depending on whether θ/π is rational or not, the dynamics is different. The set Δ' usually displays a ''fractal'' structure, consisting of complicated patterns, repeated at different scales. In order to better understand this structure, we studied the box-counting and the correlation dimension of the set Δ' for θ/π irrational and the complexity of the language for some rational and irrational θ/π. The former case was done in the attempt to check Ashwin's conjecture that the set Δ' has positive *Lebesgue measure*; we give strong numerical evidence that the *box-counting dimension* is 2. Since piecewise isometries have zero topological entropy, the complexity function is a useful tool to illustrate the combinatorial and arithmetic properties of the dynamics. For our map we find a low-order polynomial complexity; in some cases even (piecewise) linear complexity. In the last section we will develop a general scheme, first introduced in Refs. 2 and 3, to conjugate piecewise isometries on a torus with discretized rotations on a multidimensional lattice. The algebraic degree of the rotation angle is related to the dimension n of the torus: angles of higher algebraic degree tend to produce more complicated systems, and this could explain the different behavior encountered in the growth of the complexity function.

II. NOTATION

A. Preliminaries

We will follow the notation of Ref. 8. Consider the two-dimensional torus $\Omega=(\mathbb{R}/\mathbf{Z})^2$, where $\mathbf{Z}$ is the $\mathbb{Z}^2$ lattice centered at the origin: $\mathbf{Z}=\mathbb{Z}^2-(\frac{1}{2},\frac{1}{2})$. We will study the map induced by the matrix

$$T(x)=M_\tau x \bmod \mathbf{Z} \quad \text{for } M_\tau=\begin{pmatrix} 0 & 1 \\ -1 & \tau \end{pmatrix}.$$

The eigenvalues of M_τ are $\lambda_{1,2}=(\tau\pm\sqrt{\tau^2-4})/2$. If $|\tau|\leqslant 2$, the eigenvalues are on the unit circle and the matrix is elliptic. Moreover, if $\tau\notin\mathbb{Z}$, then M_τ does not preserve the lattice, and iterates of $T(x)$ are not given by the power of M_τ. The transformation T is discontinuous on the circle $[-1/2,1/2]\times\{1/2\}$. Indeed,

$$\lim_{y\to 1/2} T(x,y)=\left(\frac{1}{2},\frac{\tau}{2}-x\right)\neq\left(-\frac{1}{2},-\frac{\tau}{2}-x\right)=\lim_{y\to -1/2} T(x,y).$$

The determinant of M_τ is 1 and T is a one-to-one transformation, so the Lebesgue measure is preserved. One can easily check that M_τ is conjugate to a rotation by a linear change of coordinates $x\mapsto Cx$, for the following matrix:

$$C=\begin{pmatrix} 1 & -\tau/2 \\ 0 & \sqrt{1-\tau^2/4} \end{pmatrix}.$$

Letting $\cos\theta=\tau/2$, we get

$$C\cdot M_\tau=R_{-\theta}\cdot C,$$

where R_θ is the rotation matrix θ. In the new coordinates, the transformation becomes

$$F_\theta(x)=R_{-\theta}x \bmod L_\theta$$

on the lattice $L_\theta=C(\mathbf{Z})$. We can identify the transformation F_θ with a piecewise rotation on a rhombus Ω_θ (cf. Ref. 8), whose vertices have coordinates

$$a=((-1+\cos\theta)/2,-(\sin\theta)/2),$$

$$a'=((1+\cos\theta)/2,-(\sin\theta)/2),$$

$$a''=((-1+\cos\theta)/2,(\sin\theta)/2),$$

$$a'''=((1-\cos\theta)/2,(\sin\theta)/2).$$

The discontinuity circle becomes the segment $\langle aa'\rangle$. We are interested in the iterations of this set. Let

$$\Delta_\theta=\bigcup_{n=-\infty}^{\infty} F_\theta^n\langle aa'\rangle.$$

In general, this set is very complicated and displays a fractal structure. Figure 1 shows an angle irrational $\sqrt{2}\pi/4$. This example will be further investigated; it also serves as a test case for our numerical algorithms.

B. Partition and coding

The set Ω_θ has a natural partition into three atoms: P_0, the set of points which remain in the rhombus under the rotation and P_{-1} and P_1, the sets of points mapped outside of the rhombus at the lower side and the upper side, respectively (see Fig. 2).

$$P_0=\{x\in\Omega_\theta | R_{-\theta}x\in\Omega_\theta\},$$

$$P_{-1}=\{x\in\Omega_\theta | (R_{-\theta}x)_2>(\sin\theta)/2\},$$

$$P_1=\{x\in\Omega_\theta | (R_{-\theta}x)_2<(-\sin\theta)/2\},$$

where $(x)_2$ denotes the second component of the vector x. Now the transformation becomes a piecewise isometry,

$$F_\theta=\begin{cases} f_{-1}=R_{-\theta}x-v & \text{if } x\in P_{-1}, \\ f_0=R_{-\theta}x & \text{if } x\in P_0, \\ f_1=R_{-\theta}x+v & \text{if } x\in P_1, \end{cases}$$

where $v=(-\cos\theta,\sin\theta)$; in Fig. 2 we can see that $v=\overrightarrow{a''a}$. We will encode orbits using the map:

$$\alpha(x)=\begin{cases} -1 & \text{if } x\in P_{-1}; \\ 0 & \text{if } \in P_0; \\ 1 & \text{if } x\in P_1. \end{cases}$$

Hence we will define the *forward itinerary*:

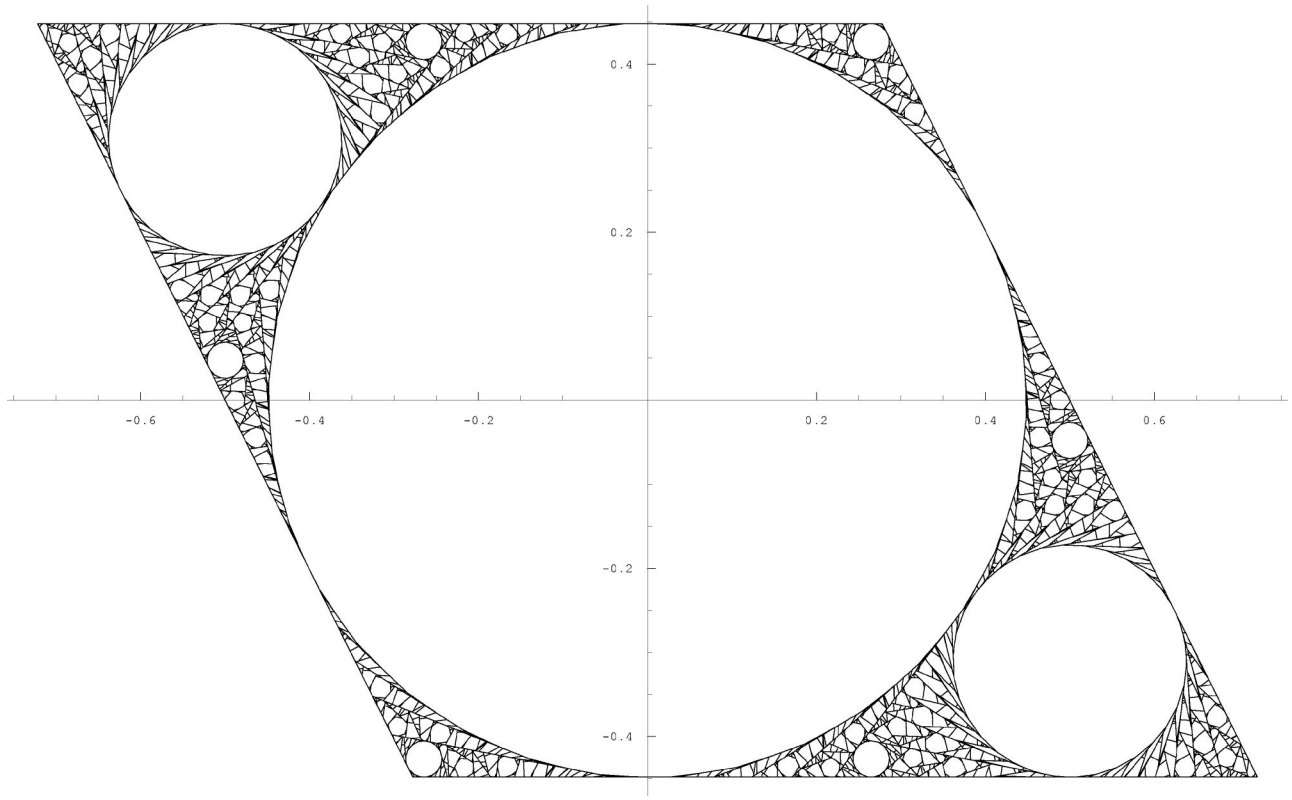

FIG. 1. The images of the discontinuity line Δ_θ for $\theta=\sqrt{2}\pi/4$.

$$\iota:\Omega_\theta \mapsto W_F := \iota(\Omega_\theta), \iota(x)=(\alpha(x),\alpha(F_\theta(x)),\ldots).$$

Note that the map ι is not injective; several points can follow the same itinerary, for example the points in the neighborhood of 0 are merely rotated by the angle θ, so their code is $(00000\ldots)$. We call a *cell* the set of all the points which follow the same itinerary. The set of cells is therefore the quotient of Ω_θ by the equivalence relation ''having the same code:''

$$x\sim y \Leftrightarrow \iota(x)=\iota(y).$$

Another way of saying this is that the set of the cells $\Sigma=\Omega_\theta/\sim$ is the collection of the connected components of the dynamical refinement $\Sigma=\bigvee_{i=0}^{\infty}F_\theta^{-i}P$. Indeed,

$$\begin{aligned} A\in\Sigma &\Leftrightarrow A=P_{\alpha_1}\cap T^{-1}P_{\alpha_2}\cap\cdots \\ &\Leftrightarrow \forall x\in A, x\in P_{\alpha_1}\cap T^{-1}P_{\alpha_2}\cap\cdots \\ &\Leftrightarrow \forall x\in A, \iota(x)=(\alpha_1,\alpha_2,\ldots). \end{aligned}$$

All points in A are equivalent, so $A\in\Omega_\theta/\sim$. On the set Σ, the map ι conjugates the map F_θ to a subshift of $\{-1,0,1\}^{\mathbb{N}}$.

Similarly, one can define the cells of order m: $\Sigma_m=\bigvee_{i=0}^{m}F_\theta^{-i}P$ which is the quotient by the equivalence relation:

$$x\sim_m y \Leftrightarrow (\iota(x))_i=(\iota(y))_i,\ \ \forall i\leqslant m.$$

Note that since the partition atoms are convex, the sets Σ_m are convex for all m as well. The topological entropy can be defined as the exponential growth rate of the number of elements of Σ_n; this is exactly the exponential growth rate of the number of n words. We can now split the torus into three main invariant sets:

(i) O is the union of the maximal open neighborhoods (called *periodic islands*) surrounding the periodic points. This is an open set, and hence of positive Lebesgue measure. Each point in O is periodic or quasiperiodic, with a periodic itinerary.

(ii) Δ_θ consists of the discontinuity line and its forward and backward images. As a countable collection of segments, its Lebesgue measure is zero.

(iii) $\Delta'_\theta=\overline{\Delta}_\theta-\Delta_\theta$, called the *exceptional set*. This set contains no periodic orbits. Its Lebesgue measure and fractal dimension are unknown, except for the examples discussed in Ref. 8.

III. DIMENSION ESTIMATES

For most angles θ, the set Δ'_θ appears to be fractal in the sense that it displays a complicated geometric structure at every scale. Only for the example $\theta=\pi/4$, the Hausdorff dimension is known exactly, and it coincides with the box-counting dimension. For other rational angles (i.e., $\theta=\pi/q$), the structure becomes more complicated as the denominator q increases, but the dimension seems to remain strictly less than 2. The irrational case displays an even more complicated structure. Calculations made in Ref. 13 seem to indicate that the dimension is 2. One of our aims is to confirm this conjecture by different methods. Namely, we carry

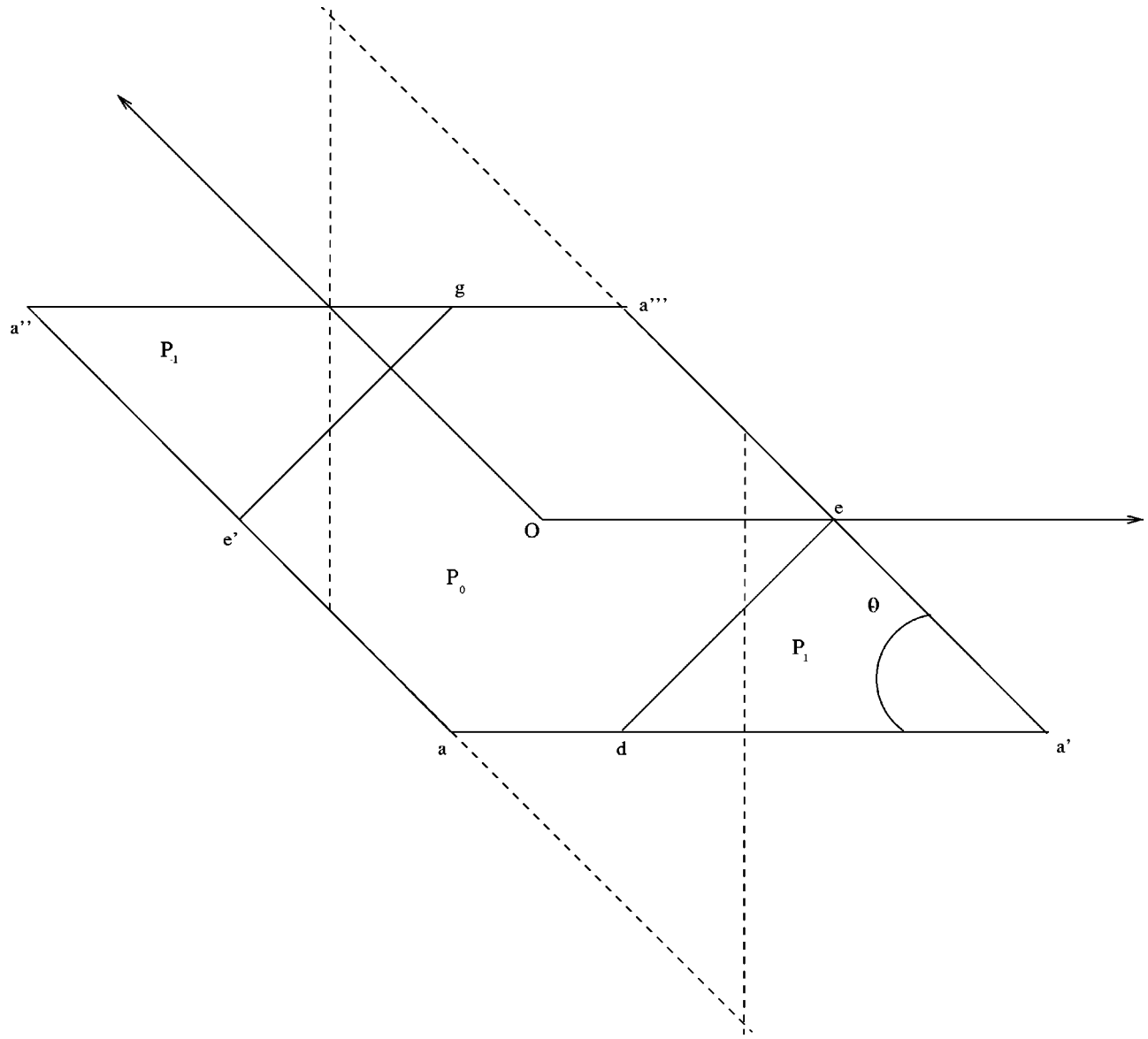

FIG. 2. The partition $\{P_0, P_1, P_{-1}\}$.

out a box-counting algorithm and we compute the correlation dimension of order 2 on an approximation of Δ_θ by a set of up to 512 million points.

Let us recall some definitions. For a bounded set $\Lambda \subset \mathbb{R}^n$, let A_ϵ be a cover of Λ by sets of diameter ϵ. Let $N(\epsilon)$ be the minimal cardinality of such a cover. If for small ϵ, $N(\epsilon)$ scales as a power law:

$$N(\epsilon) \sim \epsilon^{-d}$$

then d is defined to be the box-counting dimension of Λ. To compute the *correlation integral*, we consider a large sequence $\{x_1, \ldots, x_N\}$ of N points randomly chosen in Λ. The correlation integral is defined by

$$C(\epsilon) := \lim_{N \to \infty} \frac{1}{N^2} \#\{(i,j) \mid |x_i - x_j| \leqslant \epsilon\},$$

if the limit exists. We refer to Refs. 14 and 15 for a rigorous justification of this formula for some large class of dynamical systems. For $\epsilon \approx 0$, the correlation integral is expected to scale as

$$C(\epsilon) \sim \epsilon^{\nu},$$

then ν is called the *correlation dimension or correlation exponent* of Λ. In general one can prove that $\nu \leqslant d$. See, for example, Ref. 16. The method requires a discretization of Δ_θ. We will work with an approximation of Δ_θ obtained by iterating a set of 10 000 uniformly distributed points on the discontinuity line. Estimates will be made at various scales and on various parts of this set. Basically one considers a grid covering the window to be studied. Because of memory constraints we were unable to consider grids finer than 5000×5000. In compensation, we can make the window arbitrarily small and, with sufficiently long computation time, study arbitrarily small scales (up to machine precision of

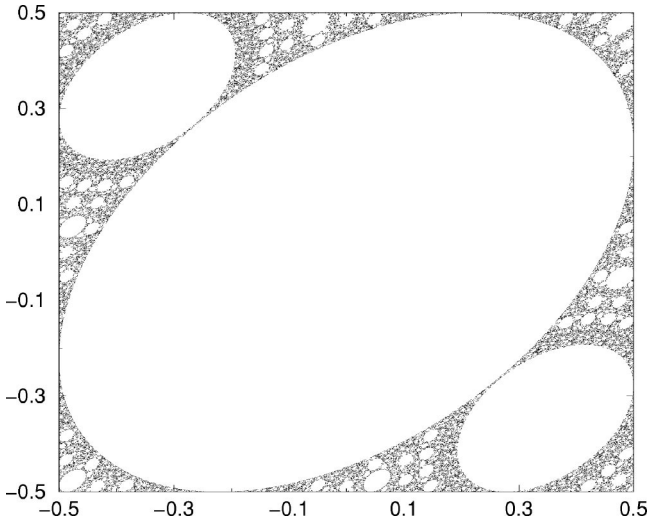

FIG. 3. The set $\overline{\Delta_\theta}$ for $\theta=\sqrt{2}\pi/4$, on which we do the dimension estimates.

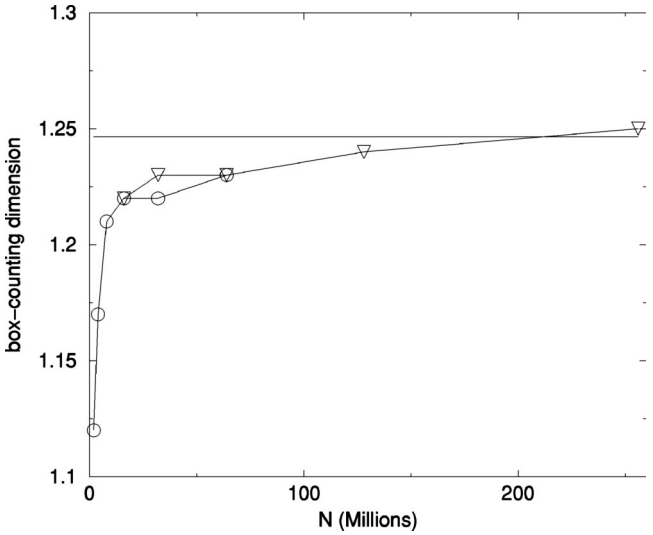

FIG. 4. Box-counting dimension for $\theta=\pi/4$. The circles, respectively, triangles correspond to scales $\epsilon=10^{-2}$, respectively, 10^{-3}, the horizontal line corresponds to the theoretical value $d=\ln(3)/\ln(1+\sqrt{2})$.

course but in fact computation time is the practical limitation). To save memory, the iterations are ''memoryless:'' each point of the discontinuity line is checked to be in the window and increments the number of hits in the cell of the grid in which it falls. In this way, we get a ''density map'' of the set. It tells us how many nonempty boxes there are. Moreover the number of points in each cell gives an estimate of the number of points separated by a distance smaller than the diameter of the cell. This gives us a way to estimate the box-counting dimension (counting the nonempty boxes) and the correlation dimension, assuming the points are uniformly distributed over the cell. This assumption is an oversimplification, but it is a necessary approximation since it is impossible to consider every possible pairs (which could be of order 10^{17}).

In order to perform concrete computations, we must fix θ. We have chosen $\theta=\sqrt{2}\pi/4$ (see Fig. 3). (Other choices seem to generate sets Δ_θ with similar structure.) The set is embedded in a unit square (see Fig. 3). As we are limited to a 5000×5000 grid, computations on the whole set constrains us to use $\epsilon\geqslant2\times10^{-4}$. These scales are quickly saturated, that is to say the values obtained stabilize early. Values of box-counting dimension for ϵ from 10^{-1} to 10^{-2} stabilize at 1.82, and for ϵ from 2×10^{-3} to 2×10^{-4} (finest grid), the value does not exceed 1.89. If we want to go to smaller scale, we are led to use a window, at the risk of making a bad choice, where dimensions could be smaller locally. The window is chosen so that it does not contain too big holes. Its side length 10^{-1}, by which we reach scales down to 10^{-5}. The return times to this window will of course become longer. Therefore going to even smaller scale, say by a factor 10, to obtain the same number of points (up to 512 million) in the window would lead to huge computation time.

In order to check the method's efficiency, some tests have been done on the case $\theta=\pi/4$ for which Hausdorff dimension is theoretically known to be $\ln(3)/\ln(1+\sqrt{2})$. The box-counting results are collected in Fig. 4, where each point is an estimate for a fixed number of points and for a fixed scale. The circles indicate scales ϵ from 10^{-2} to 10^{-3}, and the triangles ϵ from 10^{-3} to 10^{-4}. The plot shows that we find the theoretical value with reasonably good accuracy. The same is done for $\theta=\sqrt{2}\pi/4$ in Fig. 5. Here the convergence is very slow, with scales down to 10^{-5} and the number of points up to 10^9 in the window. The box-counting dimension hardly exceeds 1.95. Results for correlation dimension are more suggestive, we have a faster value around 1.97, as shown in Fig. 6. Furthermore, one can ask if the set shows inhomogeneities in its fine fractal structure. In other words, does the set display *multifractal* features? One way to investigate this aspect is to compute the generalized dimensions D_q (see below) and see if we obtain a multifractal spectrum. The standard way to do this is to choose a sequence of points on Λ and compute the q-correlation integral (see Refs. 16 and 17), defined as

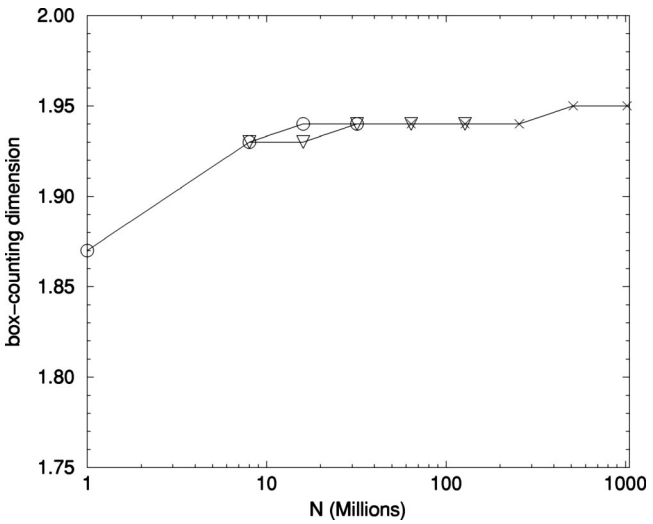

FIG. 5. Box-counting dimension approximation based on N points for $\sqrt{2}\pi/4$, here $\epsilon=10^{-2}$ for circles, 10^{-3} for triangles and 10^{-4} for crosses.

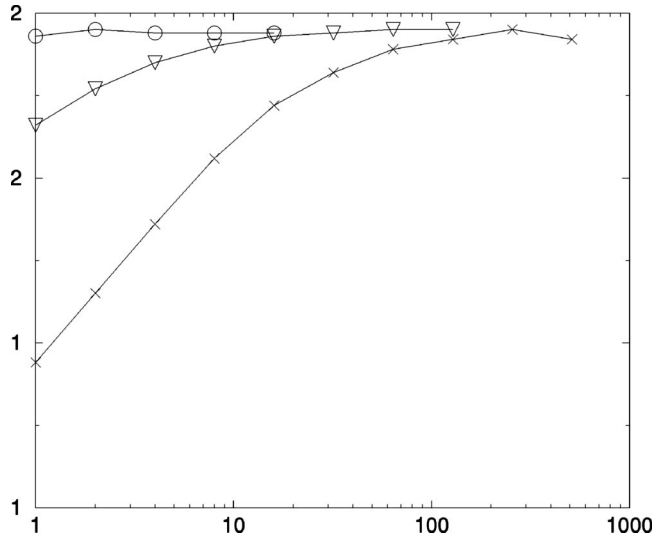

FIG. 6. Correlation dimension results for $\theta=\sqrt{2}\pi/4$. The scales are $\epsilon=10^{-2}$ for circles, 10^{-3} for triangles and 10^{-4} for crosses.

$$C^q(\epsilon)=\lim_{N\to\infty}\left(\frac{1}{N}\sum_i\left(\frac{1}{N}\sum_j\Theta(\epsilon-|X_i-X_j|)\right)^{(q-1)}\right)^{1/(q-1)},$$

where Θ denotes the Heaviside function. If the limit exists, then the generalized dimensions are defined as

$$D_q=\lim_{\epsilon\to 0}\frac{\ln C^q(\epsilon)}{\ln\,\epsilon}.$$

The Legendre transform of $D_q\cdot(q-1)$ gives the Hausdorff dimension of the level sets with a prescribed local scaling of the natural invariant measure, cf. Ref. 14. We notice that for $q=2$, the integral $C^2(\epsilon)$ is just the number of couples of points separated by a distance less than ϵ, as above.

In order to compute this quantity in general, we will refine the method described above. Instead of storing only the number of points in each cell, we will recall the points themselves but each in their respective cells. In this way, we obtain a list of points for each cell. To save computation time, we will restrict the computation of the quantity $\Theta(\epsilon-|X_i-X_j|)$ for a given X_i, to the X_j in the surrounding cells only. This method computes exactly the quantities C^q but needs much more memory than the previous one. As a consequence, we cannot use too many points on the attractor: we used 5 million points for scales ranging from 10^{-2} to 10^{-3}. Our experiments show that D_q is constant 2 (within the ranges of our computation accuracy), which gives strong numerical evidence that Δ'_θ has a unifractal structure, uniformly over Δ'_θ and over scales.

IV. COMPLEXITY

Except for the special case studied in Ref. 8, the language produced by the dynamical system F_θ is not understood. We already know that the entropy is 0 (cf. Ref. 11). In this section, we will investigate the complexity of the language numerically. We denote by $p(n)$ the number of subwords of length n appearing in the language, which is equal to the number of cells of order n. The topological entropy of the shift is the exponential growth rate of $p(n)$; it coincides with the topological entropy of the system T itself. Hence $p(n)$ grows subexponentially.

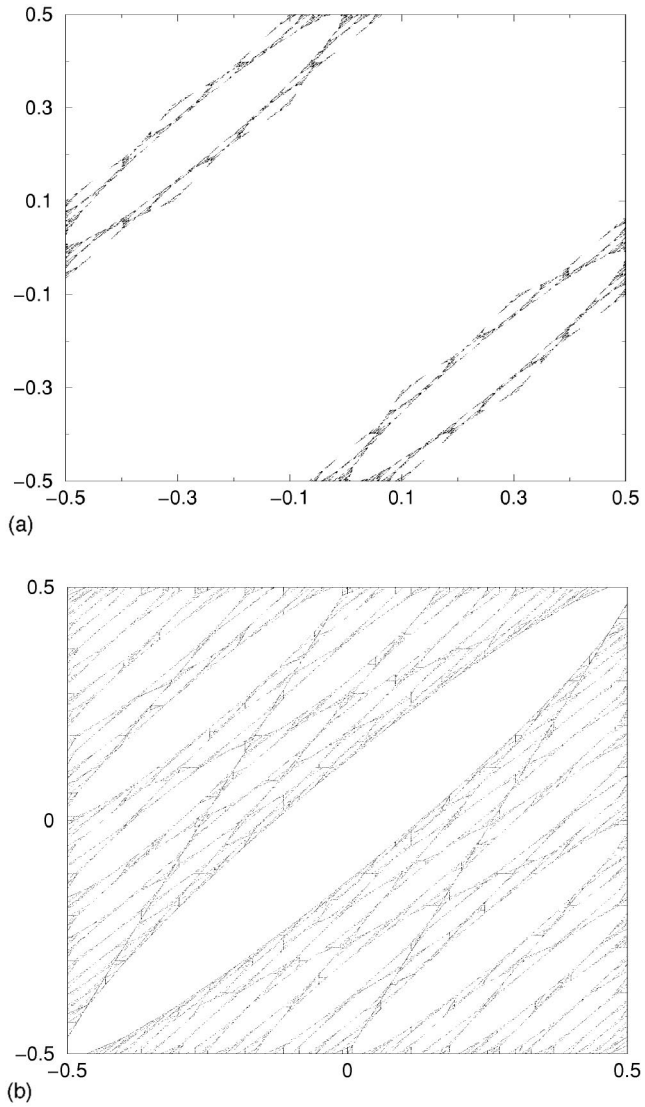

FIG. 7. Plot (a) shows an aperiodic orbit for $\theta=\pi/12$ which is not dense in the closure of the discontinuity set $\overline{\Delta_\theta}$ shown on the plot (b).

We will study several angles, and we will see that the complexity varies, depending on the rationality of the angle. We can compute complexity in two different ways, by counting subwords in the language, and by counting cells. However, the first method is not very practical. One can only compute the number of subwords of one (or finitely many) very long words, but in general, we cannot be sure that this word contains all possible subwords of the language. There is no guarantee that the point whose itinerary is used to count the subwords visits all possible cells. In general, the dynamics on the exceptional set seems to be nonminimal. Figure 7 shows an example of an infinite but nondense orbit in the exceptional set.

In order to estimate the complexity of the map in a reliable way, we prefer to compute the n cells themselves ex-

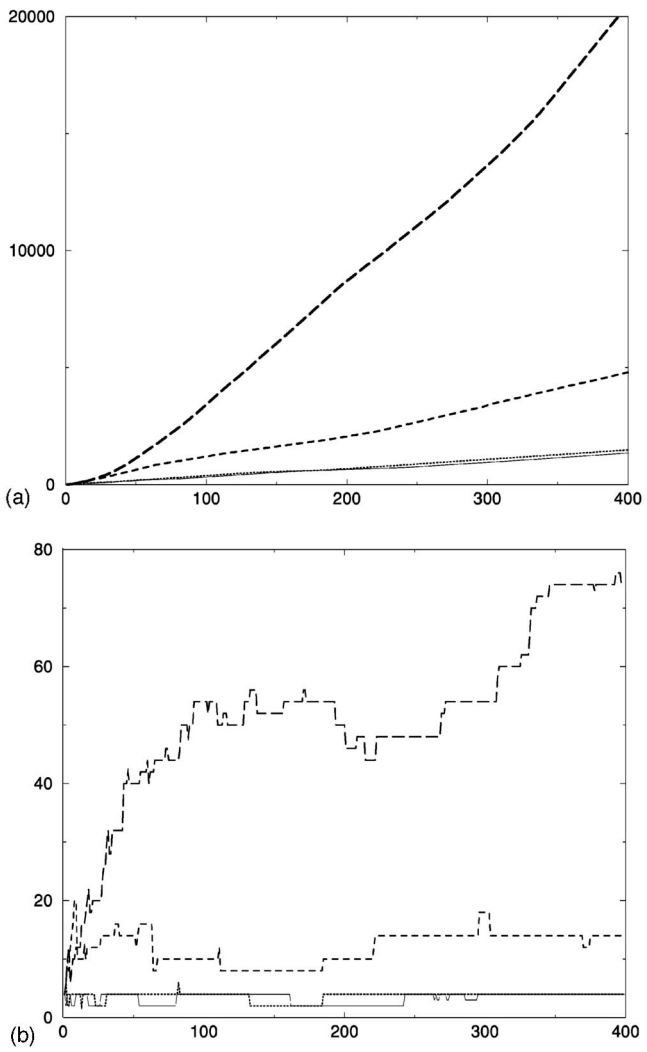

FIG. 8. Plot (a) shows the complexity function $p(n)$ for $\theta=\pi/q$, $q=4,5,6,7$ (bottom to top). In plot (b) we have the forward differences $p(n)-p(n-1)$ for the same angles.

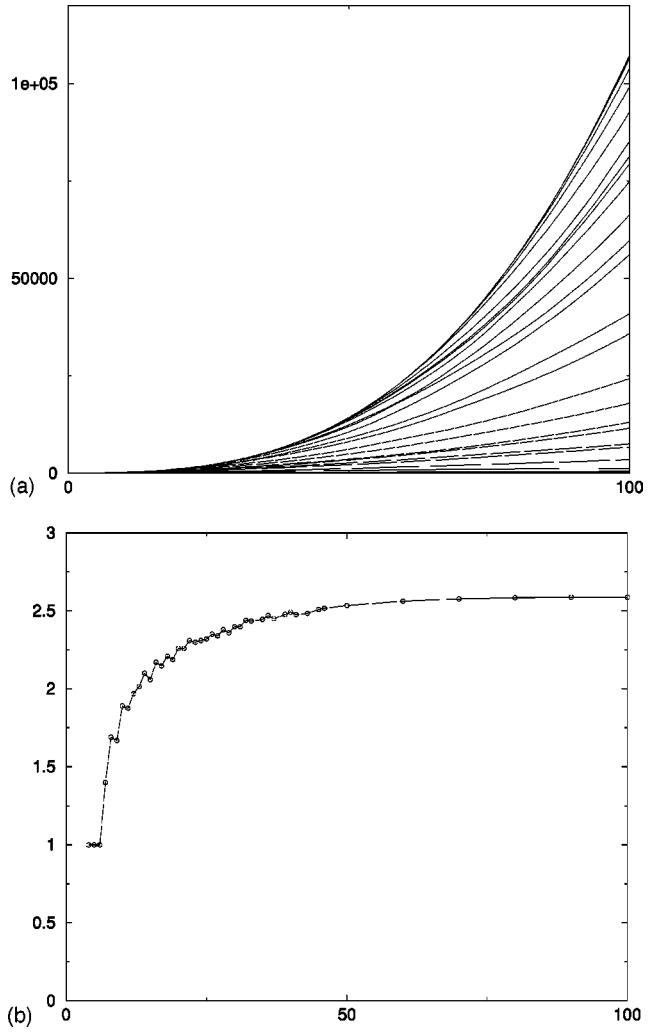

FIG. 9. Plot (a) shows the complexity function $p(n)$ for $\theta=\pi/q$. The curves increase for increasing q. In plot (b), the exponent of the corresponding power law versus q, for $q=4,\ldots,100$.

plicitly, and just count them. Computing the n cells involves computing every intersection in the dynamical refinement, that is to say, intersections of polygons. We have implemented the code in C, using the library GPC (for Generic Polygon Clipping[18]), which implements an extension of the Vatti algorithm (see Ref. 19).

Basically, we have considered four types of angles.

(1) Rational angles of the form $\theta=\pi/q$ for $q=4,5,\ldots$.
(2) Rational angles $p\pi/q$, where p/q are convergents (in the continued fraction expansion) of two ''very'' irrational numbers: the golden mean $\theta=(\sqrt{5}-1)\pi/2$ and $\theta=\sqrt{2}\pi$.
(3) Quadratic irrational angles, namely $\theta=(\sqrt{5}-1)\pi/2,\sqrt{2}\pi/4,\sqrt{3}\pi/5$.
(4) A cubic irrational angle: $\theta=2^{1/3}\pi/4$ and some rational rotation numbers τ, namely $\tau=1/2$ and $\tau=1/5$.

Several interesting things can be noticed for the first type. Indeed, as shown in Figure 8, for $q=4,5,6$ the plots of $p(n)$ versus n consist of broken lines, and the curve of *forward differences* $p(n)-p(n-1)$ are roughly constant. For $p=7$ however, where the complexity displays a shape similar to the previous cases, the plot consists of pieces of curves rather than pieces of lines. Moreover the forward differences plot is not monotone (yet roughly increasing) and very different from the previous cases. For $\pi/8$ we did not find the piecewise linear behavior within the depth of recursion used. Here one can notice that the real numbers $2\cos(\pi/q)$ in the transformation matrix are always algebraic. For $q=4,5,6$, they are quadratic, and we see a common piecewise linear behavior for all of these angles. If $n=7$, then $2\cos(\pi/q)$ is a cubic number, and we find a different, piecewise ''smooth,'' behavior for this angle. The next case, $q=8$ gives an algebraic number of degree 4, and the corresponding plot does not exhibit any piecewise behavior anymore. This suggests a relationship between the complexity of the transformation and the algebraic degree of its parameters. Some support for this suggestion emerges from the work of Vivaldi *et al.*,[2,3] see Sec. V, where the algebraic degree plays a central role. In any case, the complexity tends to increase with denominator q. For $q>7$, the curves computed seem to be best fit (in the sense of least squares) by a power law. Figure 9(a) displays

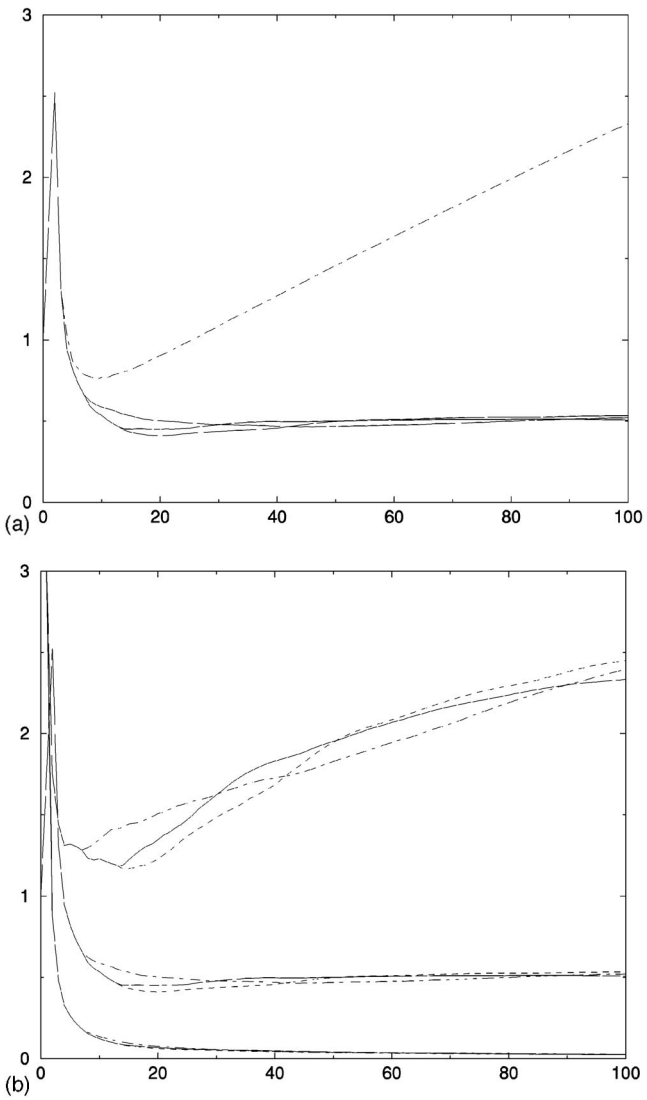

FIG. 10. Plot (a) shows a comparison between the complexity for irrational angles [solid $\theta=(\sqrt{5}-1)\pi/2$, dotted $\theta=\sqrt{2}\pi/4$ and dashed curves $\theta=\sqrt{3}\pi/5$] and rational $\theta=\pi/50$ (dotted–dashed curve). Plot (b) shows normalizations $p(n)/f(n)$ for irrational cases, $\theta=(\sqrt{5}-1)\pi/2,\sqrt{2}\pi/4,\sqrt{3}\pi/5$ for dotted–dashed, solid and long-dashed curves respectively; from top to bottom, normalizations are done by $f(n)=n^2,n^2\ln(n),n^3$.

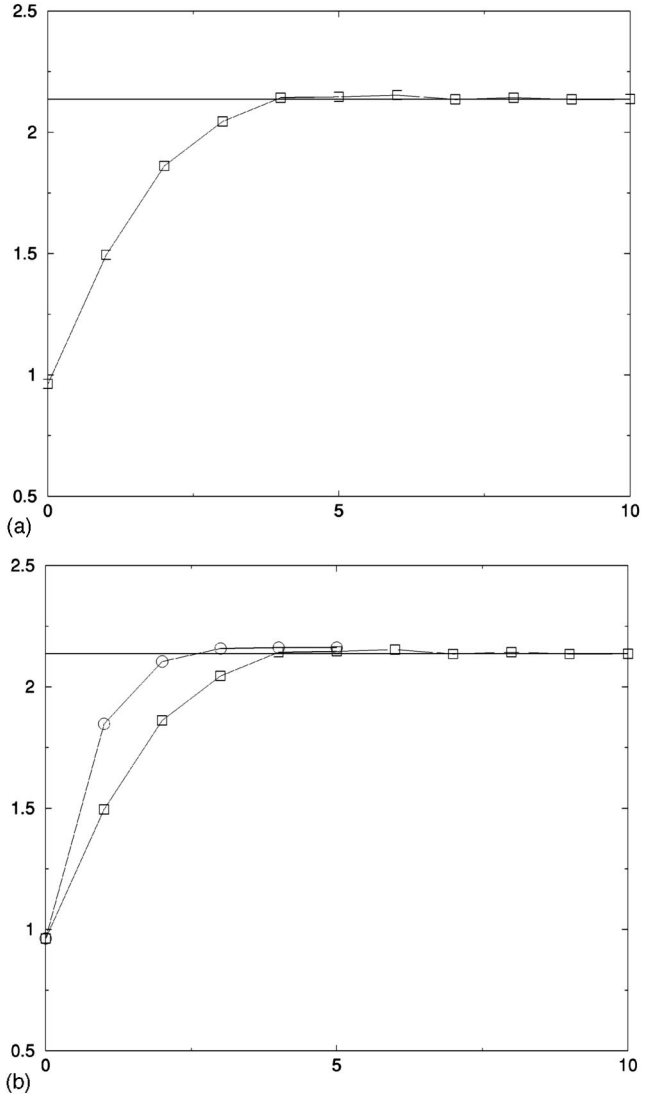

FIG. 11. Plot (a) illustrates on the growth of the regression exponent (vertical axis) of the complexity of $\pi p_n/q_n$ with respect to n (horizontal axis) when $p_n/q_n\to(\sqrt{5}-1)/2$. The horizontal solid line shows the exponent for the ''true'' irrational angle. Plot (b) shows the same curve together with the corresponding approximations for $\pi p_n'/q_n'\to\pi\sqrt{2}$ (curve with circles). Both curves seem to have the same limit.

a set of curves for increasing q. We can see that the curves converge; the limit curve is shown as a dashed line. The corresponding exponents of these power laws are shown in Fig. 9(b): they accumulate at the value ≈ 2.59. (We used 100 iterates for largest q while up to 400 iterates for the smallest.) Based on some stability tests, an error of roughly 5% is expected.

Since the complexity increases with q, and the polygons approximate the ellipses (cf. Fig. 3) better as q increases, one would expect the complexity for irrational angles to be an upper bound for the complexity of any rational case. An example quickly shows that this is not the case. Figure 10(a) shows three irrational cases together with the limit curve (described above), corresponding to π/q for large q. For all the irrational cases we studied [namely $\theta=(\sqrt{5}-1)\pi/2,\sqrt{2}\pi/4,\sqrt{3}\pi/5$], the regression exponents are very close to each other. Moreover, considering irrational angles better approximated by rationals, like $\sqrt{7}$ or $\sqrt{11}$ does not suggest to us any connection between the complexity and these arithmetic properties of the parameter.

We compared the complexity of F_θ, for irrational angles $\theta=\sqrt{2}\pi$ and $\theta=(\sqrt{5}-1)\pi/2$, to the complexity of F_θ for approximating rational angles $\theta=\pi p_n/q_n$, i.e., p_n/q_n are the convergents in the continued fraction expansion. The regression exponents turn out to grow with n to a limit; this limit is very close to the regression exponent of the irrational angle. For both irrationals, the exponents are almost the same; the differences cannot be seen in the accuracy of Fig. 11). We note that the exponents for the convergents of $\sqrt{2}$ converge approach faster than the ones for the golden mean. This confirms that $\sqrt{2}$ is indeed better approximated by rationals than $(\sqrt{5}-1)/2$.

In addition to a power law, we tried different kinds of normalizations, i.e., instead of plotting $p(n)$ versus n, we

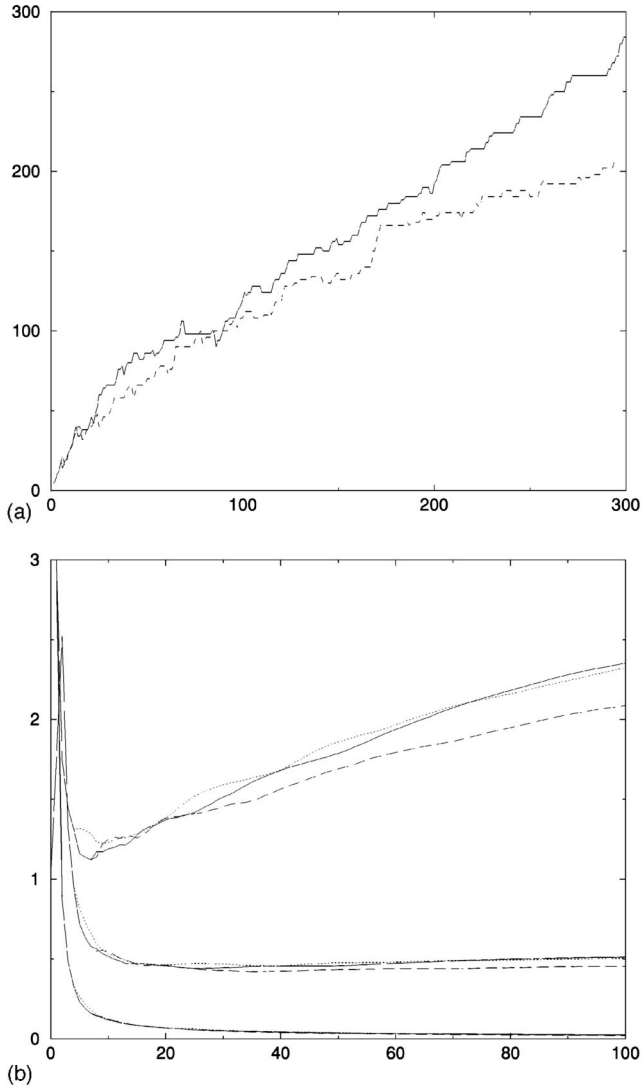

FIG. 12. Plot (a) shows the differences $p(n)-p(n-1)$ for the complexity function of the angles $\theta=\pi/8$ (solid curve) and $\theta=\pi/9$ (dashed curve). Plot (b) shows the normalized complexity functions of three irrational (w.r.t. π) rotations, namely for rotation numbers $\tau=1/2$ (long-dashed curve), $\tau=1/5$ (solid curve) and for a cubic irrational $\theta=2^{1/3}\pi/4$ (dotted curve), normalized by $f(n)=n^2$ (top group), $f(n)=n^2\ln(n)$ (middle group) and $f(n)=n^3$ (bottom group).

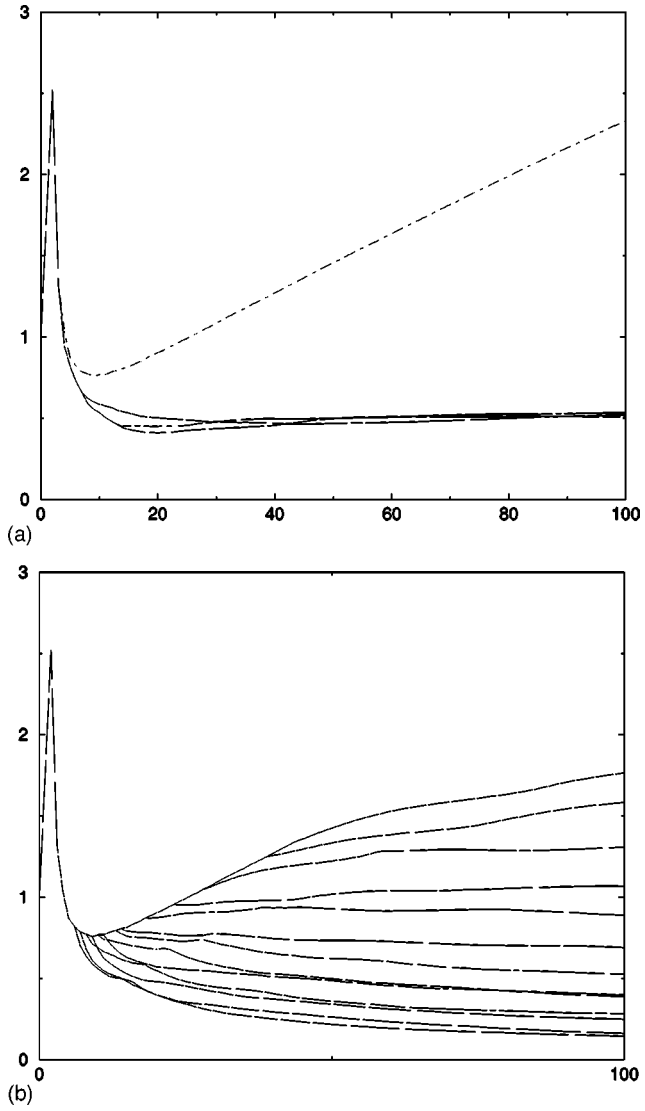

FIG. 13. Plot (a) is the normalized version of Fig. 10 (a). In plot (b) several complexity plots for rational (w.r.t. π) angles of Fig. 9(b), ranging from $\pi/4$ to $\pi/100$, are shown. Both plots are normalized by $f(n)=n^2\ln(n)$.

plot $p(n)/f(n)$ versus n for several function $f(n)\neq n^\alpha$ to see if it is more suitable than a power law n^α. For irrational angles, $f(n)=n^2\ln(n)$ seems to be a good candidate, as shown in Fig. 10(b). Here the plots of three angles, namely $(\sqrt{5}-1)\pi/2$, $\sqrt{2}\pi/4$ and $\sqrt{3}\pi/5$ are shown in solid, dashed, and long-dashed curves, respectively. From top to bottom, curves correspond to $f(n)=n^2$, $f(n)=n^2\ln(n)$ and $f(n)=n^3$. The top curves are increasing, which means that the complexity is more than quadratic. The bottom curves go to zero, which implies it is less than cubic. The middle curves seem to converge to a nonzero limit, so the complexity is $p(n)=O(n^2\ln(n))$. Figure 12(b) shows the same kind of plot as Fig. 10, but for angles having different arithmetic properties. While all the angles in Fig. 10 were quadratic irrationals (with respect to π), the angles chosen in Fig. 12 are either cubic ($\theta=2^{1/3}\pi/4$, long-dashed curve on the plot) or based on rational rotation numbers ($\tau=1/2,\tau=1/5$, solid and dotted–dashed curve, respectively); the behaviors are the same as in the previous plot, indicating that a growth of $O(n^2\log n)$ is reasonable, regardless of the fine arithmetic properties of the parameter. However, this law is not suitable for rational cases; Fig. 13(a) displays the normalized version of Fig. 10(a), whereas Fig. 13(b) displays several rational angles $\theta=\pi/q$ for increasing q, the complexity being normalized by $f(n)=n^2\ln(n)$. We see some curves increasing, some other decreasing at different rates.

V. DISCRETIZED ROTATIONS

In this section we will focus on an apparently different subject which turns out to be related to the preceding discussions. The study of the pathologies induced in dynamical systems by round-off errors is a fairly recent field of investigation, attracting an increasing amount of attention (see, for example, Refs. 2, 3, 20–26). Computer simulations almost always involve round-off errors, which affect the system in

sometimes unexpected ways. To illustrate this problem, it is helpful to track the errors precisely in simple systems. Among these systems, we can consider linear maps discretized on a uniform (= equidistant) lattice (usually, the discretization in computer arithmetic is not uniform, leading to exponential lattice). Even in this system the effects of rounding-off are far from negligible. Earlier results have been obtained by Vivaldi and his co-authors (Refs. 2, 3, 23).

In Ref. 2, a special case of discretized linear map has been studied, namely (in the notation of Ref. 2):

$$\Phi:\mathbb{Z}^2\to\mathbb{Z}^2, \quad \Phi(x,y)=(\lfloor\lambda x\rfloor-y,x),$$

for $\lambda=2\cos(2\pi/5)=(1-\sqrt{5})/2$. The key argument is that this system is isomorphic to a piecewise isometry on a dense subset of the two-torus, very similar to the ones described in the preceding sections. Moreover, the method used to describe the toral system, based on a scaling argument, is roughly the same as in Ref. 8.

Generalizations of this special result are possible for eight other values of λ, in particular $\lambda=(1+\sqrt{5})/2$ (corresponding to a rotation by $\pi/5$) and $\lambda=\sqrt{2}$ (corresponding to a rotation by $\pi/4$). Another accessible case, though computationally awkward is $\lambda=\sqrt{3}$, for which the phase portrait exhibits no clear self-similarity.

In all the mentioned cases, λ is a quadratic integer, implying that the dynamics for the so-called ''localized map'' takes place in a two-dimensional torus. The generalization of this fact is the aim of Ref. 3, where it is shown that higher degree algebraic numbers lead to higher dimensional tori.

Our interest rather concerns torus maps, so in the following sections, we will start from a torus map and show that an isomorphism can be found with a discretized map on an (eventually) multidimensional lattice, mirroring what is done in Ref. 3 in a more elementary way. This isomorphism enables us to carry properties from one system to the other. For example, it immediately connects the conjecture of the denseness of elliptic islands for toral automorphisms to the conjectured boundedness of orbits for discretized rotations. Second, as we observed in the preceding section, the complexity of the toral map $x\mapsto M_\tau x(\mathrm{mod}\ \mathbb{Z})^2$ seems to depend on the algebraic degree of $\tau=2\cos\theta$, where θ is the rotation angle. The above isomorphisms maps a dense subset $\tilde{E}_\tau\times\tilde{E}_\tau$ of the torus (see below) to the $2d-2$-dimensional lattice on which the discretized linear map acts. Although we do not pretend to have a proof, it can be expected that complexity of discretized linear maps increases with the dimension of the lattice.

Third, as observed in Refs. 8 and 2, the process of generating periodic orbits on the torus by a renormalization technique, can be translated to produce the periodic orbits on the discretized lattice by a substitution scheme. Moreover, for several cases, the shapes of the periodic orbits of the discretized rotation can be recovered by a substitution process not unlike the Koch snowflake construction. The dimension of the limit shape turns out to be equal to the dimension of the exceptional set, see Ref. 2.

A. Quadratic case

For the sake of simplicity we will deal with a map slightly different from the one described above. Namely, let

$$T(x)=M_\tau x \ \mathrm{mod}\ \mathbb{Z}^2,$$

where M_τ is the matrix given in Sec. II:

$$M_\tau=\begin{pmatrix}0 & 1\\ -1 & \tau\end{pmatrix}.$$

This map is conjugate to a rotation from the unit square $[0,1[^2$ into itself, with the same angle as before. We will further assume that τ is a quadratic integer

$$\tau^2=a\tau+b \quad \text{for } a,b\in\mathbb{Z}. \tag{1}$$

Let us define the set

$$E_\tau=\{N\tau \bmod 1;\ N\in\mathbb{Z}\}=\mathbb{Z}[\tau]\cap[0,1[,$$

where $\mathbb{Z}[\tau]$ is the smallest ring containing $\mathbb{Z}$ and τ. Unless $\tau\in\mathbb{Q}$, E_τ is a dense subset of the unit interval. We will define the one-to-one map $\Phi_0^{-1}:\mathbb{Z}\to E_\tau$ by

$$\Phi_0^{-1}:N\mapsto N\tau \bmod 1.$$

Equipped with the addition modulo 1, E_τ is a group and Φ_0 is a group isomorphism. Write $\lfloor x\rfloor=\max\{n\in\mathbb{Z}:n\leqslant x\}=x-(x \bmod 1)$ for the floor function. The aim now is to find the map $F_\tau:\mathbb{Z}^2\to\mathbb{Z}^2$ such that

$$F_\tau\circ\Phi=\Phi\circ T,$$

where $\Phi=\Phi_0\times\Phi_0$. Take $x=N\tau-\lfloor N\tau\rfloor$ and $y=M\tau-\lfloor M\tau\rfloor$. Then we get

$$F_\tau\begin{pmatrix}N\\ M\end{pmatrix}=F_\tau\circ\Phi\begin{pmatrix}x\\ y\end{pmatrix}=\Phi\begin{pmatrix}y\\ -x+y\tau\end{pmatrix}=\begin{pmatrix}M\\ -N+aM-\lfloor M\tau\rfloor\tau\end{pmatrix},$$

where in the last equality we used $\tau(M\tau-\lfloor M\tau\rfloor)=aM\tau-bM-\lfloor M\tau\rfloor\tau$. In the quadratic case, we can simplify a bit further,

$$aM-\lfloor M\tau\rfloor-N=\lfloor M(a-\tau)-N\rfloor+1=\lceil M(a-\tau)-N\rceil,$$

where $\lceil x\rceil=\min\{n\in\mathbb{Z},n\geqslant x\}$ is the ceiling function. Note that $a-\tau=-b/\tau$ is the algebraic conjugate of τ; call it τ'. Thus, F_τ can be considered as the discretized version of the linear map:

$$\hat{F}_\tau=\begin{pmatrix}0 & 1\\ -1 & \tau'\end{pmatrix}.$$

B. Remarks on the quadratic case

We saw above that the toral map based on M_τ and restricted to $E_\tau^2\subset\mathbb{T}^2$ is isomorphic to a discretized linear map F_τ. Therefore it is surprising to see that M_τ and F_τ are simultaneously elliptic only in a few cases. In infinitely many cases M_τ is elliptic while $\hat{F}_\tau$ is hyperbolic or vice versa. This follows from:

Lemma 1: Let τ and τ' be algebraically conjugate quadratic numbers. Then the matrices M_τ and $\hat{F}_\tau$ are both elliptic if and only if one of them is conjugate to a rational rotation.

Proof: First suppose that M_τ (or $\hat{F}_\tau$) is conjugate to a rational rotation. Then $|\tau|<2$ and $\tau=2\cos\theta$ for $\theta=\pi p/q$ and $p,q\in\mathbb{Z}$. Therefore

$$\cos(q\theta)=1 \quad \text{or} \quad \cos(q\theta)=-1.$$

Assume that $\cos(q\theta)=1$ (the other case is treated similarly). Then $\pi p/q$ for $p=0,2,\ldots,2(q-1)$ are the solutions of the equation $\cos(q\theta)-1=0$. By elementary trigonometry (the Euler–de Moivre formula), we can express this equation as polynomial in $\tau=2\cos\theta$:

$$P(\tau)=\left[\sum_{j=0}^{[q/2]} \binom{q}{2j}(-1)^j\left(\frac{\tau}{2}\right)^{q-2j}\left(1-\left(\frac{\tau}{2}\right)^2\right)^j\right]-1.$$

Obviously, this polynomial has degree q, and there are at most q solutions, including τ', the algebraic conjugate of τ. If $\tau'\in[-2,2]$, then M_τ and $\hat{F}_\tau$ are simultaneously elliptic, and we can use the list in the second half of the proof to conclude that $\tau'=2\cos\pi p'/q$. If $|\tau'|>2$, then any $\theta'\in\arccos(\tau'/2)$ has the form $n\pi+iw$ for some $n\in\mathbb{Z}$ and $w\neq 0$. But then $q\theta'$ has a similar form, and $\cos(q\theta')\neq 1$.

Conversely, if we have $|\tau|<2$ and $|\tau'|<2$, then as

$$\tau+\tau'=a \quad \text{and} \quad \tau\cdot\tau'=-b,$$

we have

$$|a|\leqslant|\tau|+|\tau'|<4 \quad \text{and} \quad |b|=|\tau||\tau'|<4.$$

Since $a,b\in\mathbb{Z}$, there are only a finite number of cases. Adding the constraint that τ should be irrational and real, the possibilities are

$\tau=2\cos(\theta_1)$	$\tau'=2\cos(\theta_2)$	θ_1	θ_2
$-\frac{1}{2}(\sqrt{5}+1)$	$\frac{1}{2}(\sqrt{5}-1)$	$6\pi/5$	$2\pi/5$
$-\sqrt{2}$	$\sqrt{2}$	$3\pi/4$	$\pi/4$
$-\sqrt{3}$	$\sqrt{3}$	$7\pi/6$	$\pi/6$
$\frac{1}{2}(1-\sqrt{5})$	$\frac{1}{2}(1+\sqrt{5})$	$3\pi/5$	$\pi/5$

All these cases are rational rotations, and the proof is complete.

This set of conjugated elliptic systems has been studied systematically in Ref. 23. If both systems are not both elliptic, the isomorphism can still provide useful insights. For example, if M_τ is elliptic and $\hat{F}_\tau$ hyperbolic, it is surprising to find the complexity of a hyperbolic system in a subset E_τ^2 of the torus. On the other hand, if $\hat{F}_\tau$ is elliptic and M_τ is hyperbolic, then the boundedness of all orbits of F_τ (this is an important question; there is only partial numerical evidence for boundedness of orbits) yields that E_τ^2 consists of periodic points. This would give a more precise proof than Ref. 27 of the existence dense set of periodic points for these hyperbolic discontinuous toral maps. We mention that in Ref. 28, a different approach was taken to study the discretized rotations F_τ for $\tau\in\mathbb{Q}$.

C. Higher degree cases

The result from the preceding section extend to higher degree cases, that is to say when τ is an algebraic integer of degree n. Here we shall describe the case $n=3$, the other cases being straightforward, though with more tedious computations. Suppose

$$\tau^3=a\tau^2+b\tau+c, \quad \text{for } a,b,c\in\mathbb{Z},$$

and let

$$\widetilde{E}_\tau=\{M\tau^2+N\tau \bmod 1;\ M,N\in\mathbb{Z}\}.$$

This time $\Phi_0^{-1}:\mathbb{Z}^2\to\widetilde{E}_\tau$ defined by

$$\Phi_0^{-1}:(M,N)\mapsto M\tau^2+N\tau \bmod 1$$

is a group isomorphism. Then $\Phi=\Phi_0\times\Phi_0$ conjugates T restricted to $\widetilde{E}_\tau^2$ to a map F_τ from $\mathbb{Z}^4$ onto itself. To find the expression of F_τ we are led to consider the following map from $f:\widetilde{E}_\tau\to\widetilde{E}_\tau$:

$$f:z\mapsto\tau z \bmod 1.$$

For $z\in\widetilde{E}^2$, $z=M\tau^2+N\tau \bmod 1$ we have

$$\begin{aligned}
f(z)&=\tau(M\tau^2+N\tau-\lfloor M\tau^2+N\tau\rfloor)\bmod 1\\
&=M(a\tau^2+b\tau+c)-\tau\lfloor M\tau^2+N\tau\rfloor+\tau^2N \bmod 1\\
&=\tau^2(Ma+N)+\tau(bM-\lfloor M\tau^2+N\tau\rfloor)+Mc \bmod 1\\
&=\tau^2(Ma+N)+\tau(bM-\lfloor M\tau^2+N\tau\rfloor)\bmod 1\\
&=\tau^2(Ma+N)+\tau(\lceil bM-M\tau^2-N\tau\rceil)\bmod 1.
\end{aligned}$$

If z_1 and z_2 are in E_τ the map T becomes

$$\begin{aligned}
T\begin{pmatrix}z_1\\z_2\end{pmatrix}&=\begin{pmatrix}z_2\\ f(z_2)-z_1\bmod 1\end{pmatrix}\\
&=\begin{pmatrix}M_2\tau^2+N_2\tau\\ \tau^2(M_2a+N_2-M_1)\\ +\tau(bM_2-\lfloor M_2\tau^2+N_2\tau\rfloor-N_1)\bmod 1\end{pmatrix}.
\end{aligned}$$

Therefore,

$$F_\tau\begin{pmatrix}M_1\\N_1\\M_2\\N_2\end{pmatrix}=\Phi\circ T\begin{pmatrix}z_1\\z_2\end{pmatrix}=\begin{pmatrix}M_2\\N_2\\M_2a+N_2-M_1\\bM_2-\lfloor M_2\tau^2+N_2\tau\rfloor-N_1\end{pmatrix},$$

which can also be considered as the discretization (by the ceiling function) of the linear map

$$\hat{F}_\tau=\begin{pmatrix}0&0&1&0\\0&0&0&1\\-1&0&a&1\\0&-1&b-\tau^2&-\tau\end{pmatrix}.$$

In general, if τ is an algebraic integer of degree n, then $\Phi(E_\tau^{n-1})$ is the $2(n-1)$-dimensional integer lattice, and restricted to E_τ^{n-1}, T is conjugate to the map F_τ, which is the discretized (by the ceiling function) version of the linear map:

$$\hat{F}_\tau=\begin{pmatrix}0&\mathrm{Id}\\-\mathrm{Id}&A\end{pmatrix},$$

where Id is the $n-1$ dimensional identity matrix, and the matrix A expresses the map f; it has the form

$$A=\begin{pmatrix} a_{n-1} & 1 & \cdots & 0 \\ a_{n-2} & 0 & \ddots & 0 \\ \vdots & \vdots & \ddots & \vdots \\ a_2 & \cdots & 0 & 1 \\ a_1-\tau^n & -\tau^{n-1} & \cdots & -\tau \end{pmatrix}.$$

D. Examples

1. Case $\theta=\pi/4$

This case is one of the simplest nontrivial cases, fully understandable both by the ''discrete rotation side'' (similar to the case solved in Ref. 2) and the ''toral rotation side'' (similar to the case studied in Ref. 8). Here $\tau=\sqrt{2}$, the matrix of the linear map to be discretized takes the form

$$\hat{F}=\begin{pmatrix} 0 & 1 \\ -1 & -\sqrt{2} \end{pmatrix},$$

which is, by a simple shear, conjugate to a rotation with angle $3\pi/4$. The discretized map leads to a very interesting behavior and invariant sets, reminiscent of ''elliptic islands'' in Hamiltonian dynamics, see Fig. 14. These pictures show the iterates of $\mathbb{Z}\times\{0\}$, which corresponds to a dense subset of the iterates of the discontinuity for the toral map (shown in Fig. 15). Properties of these two sets and in general of these two systems are closely related.

2. Case $\theta=\pi/7$

This is the first cubic case, and from both points of view, it is little understood. The number $\tau=2\cos(\pi/7)$ is an algebraic integer satisfying the polynomial equation

$$\tau^3=\tau^2+2\tau-1.$$

So the linear map to be discretized over $\mathbb{Z}^4$ is the following:

$$\hat{F}_\tau=\begin{pmatrix} 0 & 0 & 1 & 0 \\ 0 & 0 & 0 & 1 \\ -1 & 0 & 1 & 1 \\ 0 & -1 & 2-\tau^2 & -\tau \end{pmatrix}.$$

Its eigenvalues are $\{e^{i3\pi/7},e^{-i3\pi/7},e^{i5\pi/7},e^{-i5\pi/7}\}$, and hence the map is conjugate to a double rotation map by a suitable shear of the base vectors of $\mathbb{Z}^4$. Of course, the fact that the dynamics takes place in dimension 4 complicates the analysis, and the invariant sets are much more difficult to figure out.

VI. DISCUSSION

In this paper we investigated some open questions in the rapidly growing field of piecewise isometries. We studied a class of piecewise rotations on the square or two-torus and illustrated that the dynamics of these maps is only apparently simple. The presence of discontinuity lines, iterated backwards and forwards, generates an invariant set (the exceptional set). It has an intricate combinatorial and geometric

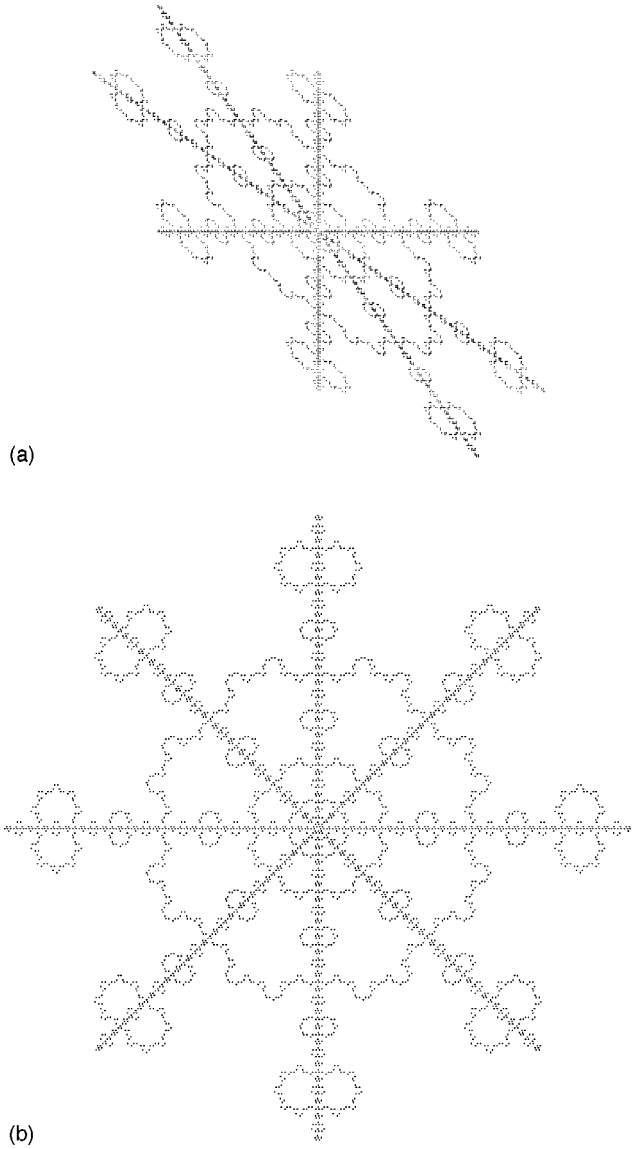

FIG. 14. Plot (a) shows the forward iterates of the set $\mathbb{Z}\times\{0\}$ by the map $F_{-\sqrt{2}}$. Plot (b) shows the same set, with the lattice sheared to make the map acting as a true rotation over the lattice.

structure, and the map acts on it as a shift on a suitable coding space. Our analysis includes at least two kinds of approaches to deal with piecewise isometries. The first, developed in Secs. II–IV, concerns the topological shape of the exceptional set Δ', and the complexity of the language that we obtain after having coded orbits according to the natural partition into the regions of continuity. We showed, with two highly reliable numerical schemes, that for irrational piecewise isometries the box-counting dimension approaches 2, thus confirming a conjecture by Ashwin.

Our computations of the complexity covers several cases (corresponding to rational and irrational angles), in an attempt to explore and classify different behaviors. Again, this was done by using very careful and precise numerical procedures. In particular, we detected a relationship between the complexity of the transformation and the algebraic degree of its parameters. In order to better understand this link, we followed a second approach, which consists of establishing

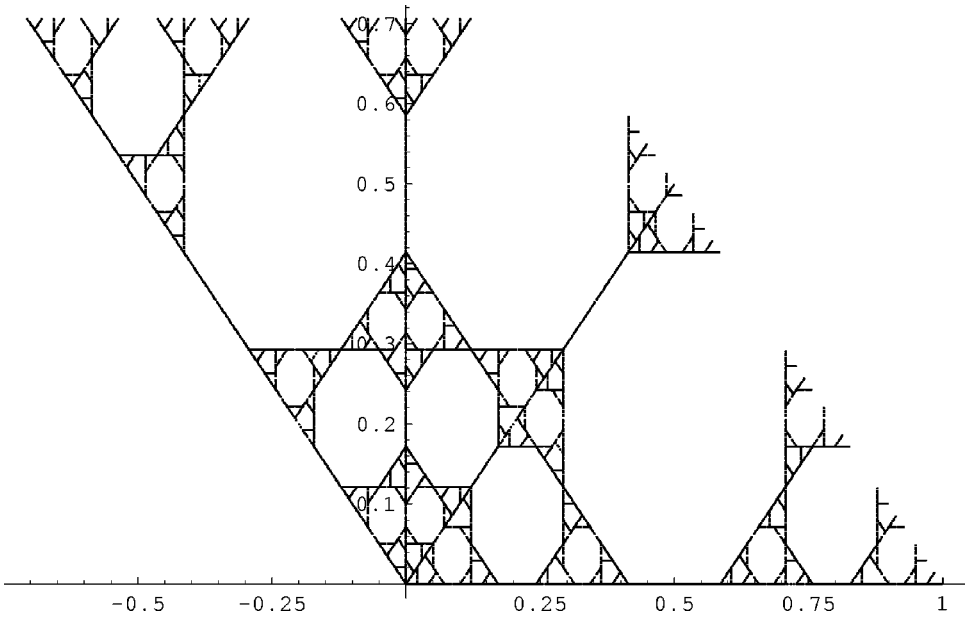

FIG. 15. The forward iterates of the discontinuity line for the toral map conjugate to $F_{-\sqrt{2}}$.

an isomorphism between the piecewise rotations and (multi-dimensional) discretized rotations. We first generalized some recent results by Vivaldi and co-workers, which are of an intrinsic interest, especially for the possibility to conjugate elliptic and hyperbolic dynamics, as we pointed out in Sec. V. It is also interesting to note that these results seem to contradict a conjecture made by Ashwin *et al.* in Ref. 29. In that paper, the planar piecewise isometries based on convex polygons were expected to have a complexity at most quadratic while we exhibited polynomial exponents significantly greater for our case.

Coming back to the relationship with complexity, we want to make the following technical observations. Recall that the piecewise isometry was characterized by a parameter θ. The fact that $\theta=2\cos(\pi/q)$ for $q=4,5,6$ are quadratic implies that the discretized rotation takes place on a two-dimensional lattice; they have a common phase space and a common complexity behavior. Numbers of higher algebraic degree require higher dimensional lattices: if θ is of degree d, then the lattice is of dimension $2(d-1)$. This increase of dimension is parallel to the increase of the complexity discussed in Sec. IV.

Rigorous mathematical methods to substantiate the numerical conclusions are still elusive. This is another interesting and promising direction in the understanding of piecewise isometries.

ACKNOWLEDGMENTS

We thank P. Ashwin, A. Goetz, P. Hubert, and F. Vivaldi for useful discussions. H.B. was supported by the University of Toulon, the Royal Netherlands Academy of Arts and Sciences (KNAW) and the Van Gogh program of the Netherlands Organization of Scientific Research (NWO).

[1] L. Chua and T. Lin, ''Chaos in digital filters,'' IEEE Trans. Circuits Syst., I: Fundam. Theory Appl. **35**, 648–658 (1988).
[2] J. Lowenstein, S. Hatjispyros, and F. Vivaldi, ''Quasiperiodicity, global stability and scaling in a model of Hamiltonian round-off,'' Chaos **7**, 49–66 (1997).
[3] J. Lowenstein and F. Vivaldi, ''Embedding dynamics for round-off errors near a periodic orbit,'' Chaos **10**, 747–755 (2000).
[4] E. Gutkin and N. Simanyi, ''Dual polygonal billiards and necklace dynamics,'' Commun. Math. Phys. **143**, 431–449 (1992).
[5] A. Goetz, Ph.D. thesis, University of Chicago, 1996.
[6] A. Goetz, ''Dynamics of piecewise isometries,'' Ill. J. Math. **44**, 465–478 (2000).
[7] A. Goetz, ''Dynamics of a piecewise rotation,'' Continuous Discrete Dyn. Syst. **4**, 593–608 (1998).
[8] R. Adler, B. Kitchens, and C. Tresser, ''Dynamics of nonergodic piecewise affine maps of the torus,'' Ergod. Theory Dyn. Syst. **21**, 959–999 (2001).
[9] B. Kahng, ''Dynamics of symplectic piecewise affine elliptic rotation maps on tori,'' Ergod. Theory Dyn. Syst. **22**, 483–505 (2002).
[10] E. Gutkin and N. Haydn, ''Topological entropy of polygon exchange transformations and polygonal billards,'' Ergod. Theory Dyn. Syst. **17**, 849–867 (1997).
[11] J. Buzzi, ''Piecewise isometries have zero topological entropy,'' Ergod. Theory Dyn. Syst. **21**, 1371–1377 (2001).
[12] P. Ashwin, *Non-Smooth Invariant Circles in Digital Overflow Oscillations*, Proceedings of the 4th International Workshop on Nonlinear Dynamics and Electronic Systems, Sevilla, 1996, pp. 417–422.
[13] P. Ashwin, W. Chambers, and G. Petkov, ''Lossless digital filter overflow oscillations; approximation of invariant fractals,'' Int. J. Bifurcation Chaos Appl. Sci. Eng. **7,** 2603–2610 (1997).
[14] Y. Pesin, *Dimension Theory in Dynamical Systems* (University of Chicago Press, Chicago, 1997).
[15] H. Hentschel and I. Procaccia, ''The infinite number of generalized dimensions of fractal and strange attractors,'' Physica D **8**, 435–444 (1993).
[16] P. Grassberger and I. Procaccia, ''Measuring the strangeness of attractors,'' Physica D **9**, 189–208 (1983).
[17] K. Pawelzik and H. Schuster ''Generalized dimensions and entropies from a measured time series,'' Phys. Rev. A **35**, 481–484 (1987).
[18] GPC, ''A General Polygon Clipping Library, version 2.31,'' Copyright 1997–1999 Alan Murta, Advanced Interface Group, Department of Computer Science, University of Manchester.
[19] B. Vatti, ''A generic solution to polygon clipping,'' Commun. ACM **35**, 56–63 (1992).
[20] M. Blank, ''Pathologies generated by round-off errors in dynamical systems,'' Physica D **78**, 93–114 (1974).
[21] M. Blank, T. Krüger, and L. Pustylnikov, ''A KAM type theorem for systems with round-off errors,'' Universität Bielefeld, 765/3/97, 1997.
[22] P. Diamond, P. Kloeden, V. Kozyakin, and A. Pokrovskii, ''Boundedness and dissipativity of truncated rotations on uniform planar lattices,'' Math. Nachr. **191**, 59–81 (1998).

[23] K. Kouptsov, J. Lowenstein, and F. Vivaldi, ''Quadratic rational rotations of the torus and dual lattice maps,'' Nonlinearity **15**, 1795–1842 (2002).
[24] F. Vivaldi and F. Vladimirov, ''Pseudo-randomness of round-off errors in discretized linear maps on the plane,'' Int. J. Bifur. and Chaos (in press).
[25] I. Vladimirov, ''Quantized linear systems on integer lattices: Frequency-based approach, Part I,'' Center for Applied Dynamical Systems and Environmental Modeling, Deakin University, CADSEM Report 96-032, 1996, 1-37, Geelong, Victoria, Australia.
[26] I. Vladimirov, ''Quantized linear systems on integer lattices: Frequency-based approach, Part II,'' Center for Applied Dynamical Systems and Environmental Modeling, Deakin University, CADSEM Report 96-033, 1996, 1-50, Geelong, Victoria, Australia.
[27] T. Krüger and S. Troubetzkoy, ''Markov partitions and shadowing for nonuniformly hyperbolic systems with singularities,'' Ergod. Theory Dyn. Syst. **12**, 487–502 (1992).
[28] D. Bosio and F. Vivaldi, ''Round-off errors and p-adic numbers,'' Nonlinearity **13**, 309–322 (2000).
[29] P. Ashwin and X.-C. Fu, ''On the geometry of orientation preserving planar piecewise isometries,'' J. Nonlinear Sci. **12**, 207–240 (2002).